



Experimental Design for the Evaluation of Detection Techniques of Hidden Corrosion Beneath the Thermal Protective System of the Space Shuttle Orbiter

Catherine C. Kammerer¹, Janice K. Lomness², Paul E. Hintze²,
Joseph A Jacoby¹, and Richard W. Russell³

¹United Space Alliance, NASA Kennedy Space Center, Specialty Engineering and Technical Services, USK-507, Cape Canaveral, FL, 32920

²NASA Kennedy Space Center, Corrosion Technology Laboratory, KT-E, Kennedy Space Center, FL, 32899

³NASA Kennedy Space Center, NASA Orbiter Project Office, MV7, Kennedy Space Center, FL, 32899



Outline



- Problem Statement
- Current Detection Procedure
- Objective of This Study
- Approach Used For Study
- Evaluated Techniques- BSX, mm-Wave, THz
- Conclusions



Problem Statement



- The United States Space Operational Space Shuttle Fleet Consists of three shuttles with an average age of 19.7 years
- Shuttles are exposed to corrosive conditions while undergoing final closeout for missions at the launch pad and extreme conditions during ascent, orbit, and descent that may accelerate the corrosion process.
- Structural corrosion under TPS could progress undetected (without tile removal) and eventually result in reduction in structural capability sufficient to create negative margins of safety and ultimate loss of local structural capability.



Current Detection Procedure



- Thermal Protection System Components
 - Panels
 - Blankets
 - Tiles





Current Detection Procedure



- 1) Removal of Tile
- 2) Visual Inspection
- 3) Corrosion Rework (if applicable)
- 4) Corrosion Protection Reapplication
- 5) Rebonding of Tile



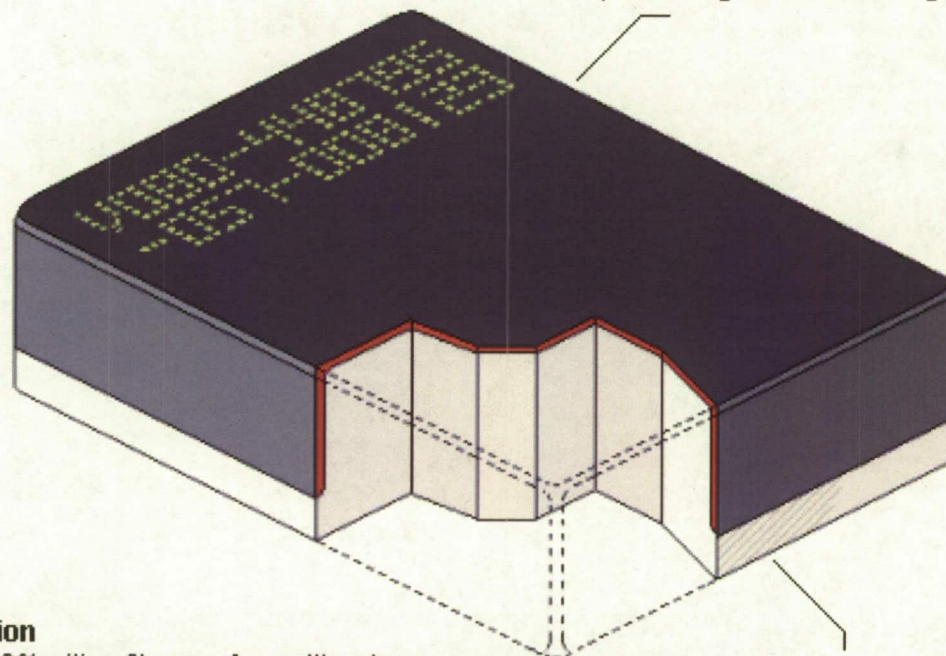


High Temperature Reusable Surface Insulation



Coating

The outer portion of a tile is covered with a black-glazed coating of borosilicate. These tiles do most of the coating job by shedding about 95% of the heat encountered. The remaining 5% is absorbed by the tile's interior, preventing it from reaching the orbiter's aluminum skin.



Composition

90% air, 10% silica fibers a few millimeters thick. The tiles feels similar to plastic foam. The silica fibers are derived from high-quality sand.

Glue

A silicon-rubber glue similar to common bathtub caulking, bonds a tile to a felt pad, that is in turn bonded to the orbiter's skin. The felt absorbs the stresses of airframe bending that could damage the tiles.



Objective of Study



- Establish the ability to detect corrosion under tile without tile removal
- Determine the key factors affecting the detection process
- Roughly Quantify the Detection threshold



Approach Used for Study



- A full factorial design with center points and replication was utilized
- The primary factors thought to affect detectability of corrosion is pit depth, diameter, or volume

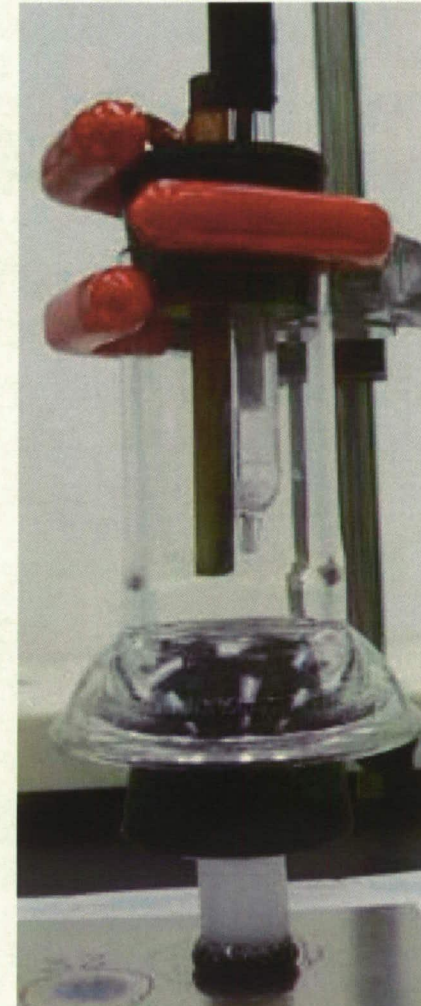
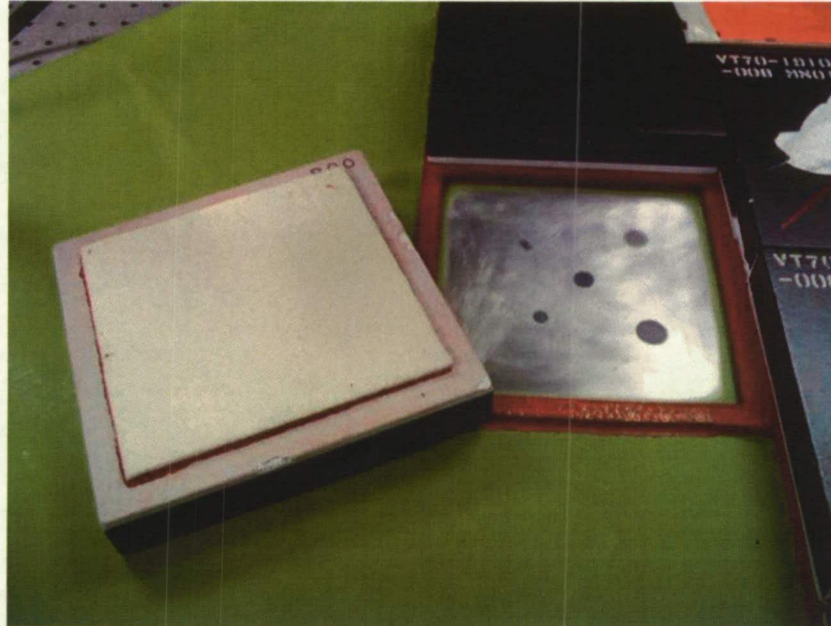
Diameter \ Depth	0.100"	0.350"	0.600"
0.003"	A		B
0.0115"		E	
0.020"	C		D



Approach Used for Study



Two test panels were fabricated by removing tile, inducing pits of various depths and diameters, rebonding the tile back in place without removing the active corrosion



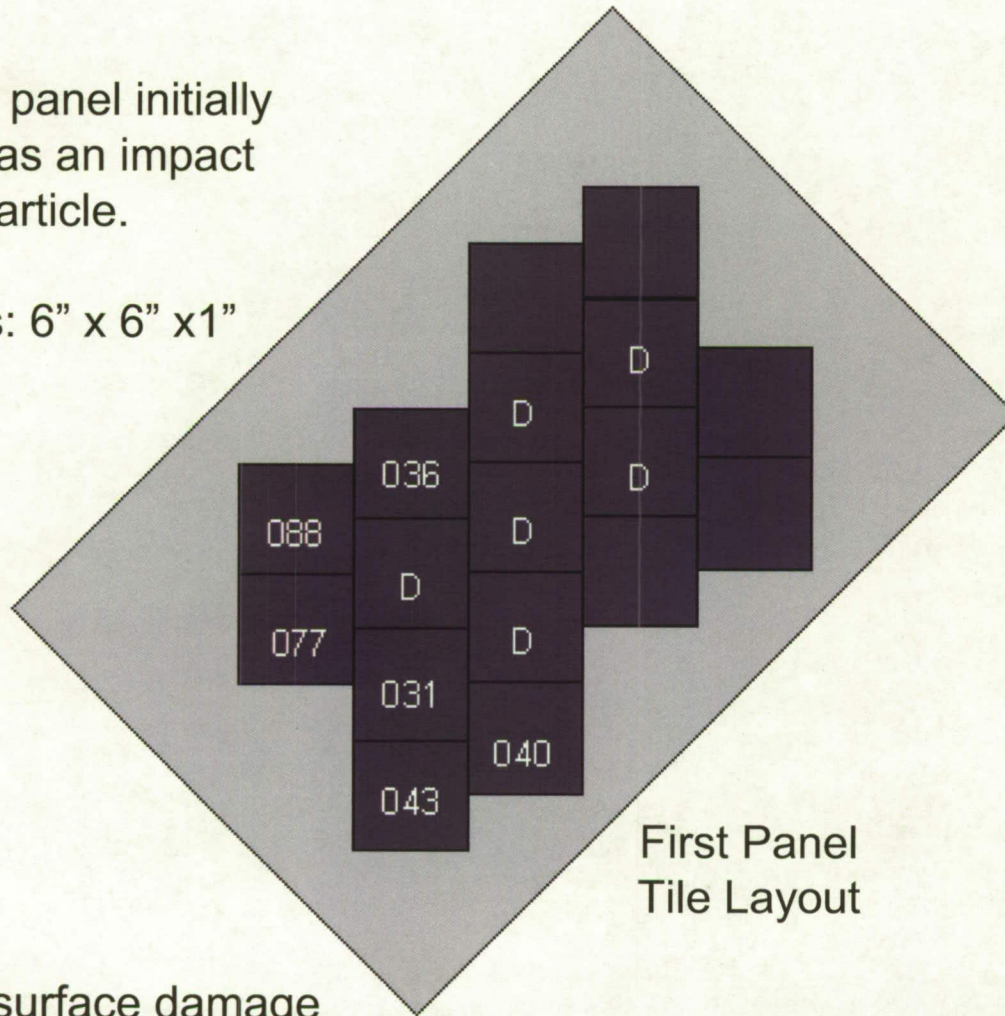


Test Panel Layout



Test panel initially use as an impact test article.

Tiles: 6" x 6" x 1"



First Panel Tile Layout

D = surface damage

On the first panel, two tiles were removed and each had five areas of corrosion induced.

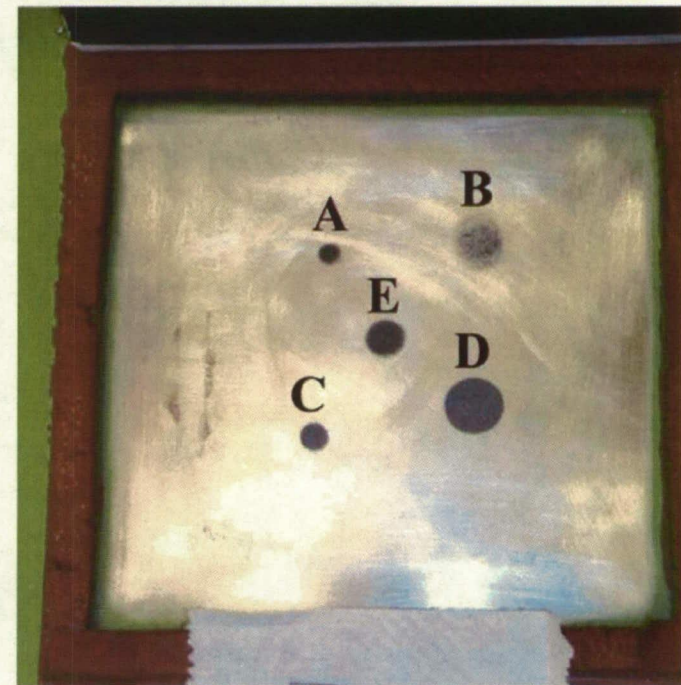
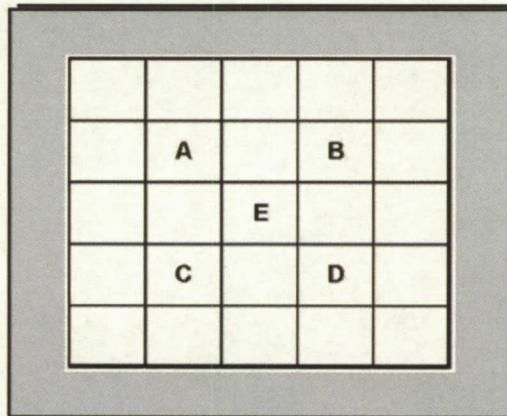
One of the tiles was re-bonded the other tile was left unattached.

This way, the substrate could be scanned with and without a tile.

Both areas of corrosion on this panel were similar in shape and depth.



Calibration Panel



Pit Location	Pit Depth (inches)	Pit Diameter (inches)
Site A	0.0031-0.0056	0.1
Site B	0.0023-0.0031	0.6
Site C	0.019-0.023	0.1
Site D	0.191-0.219	0.6
Site E	0.0132-0.0146	0.3



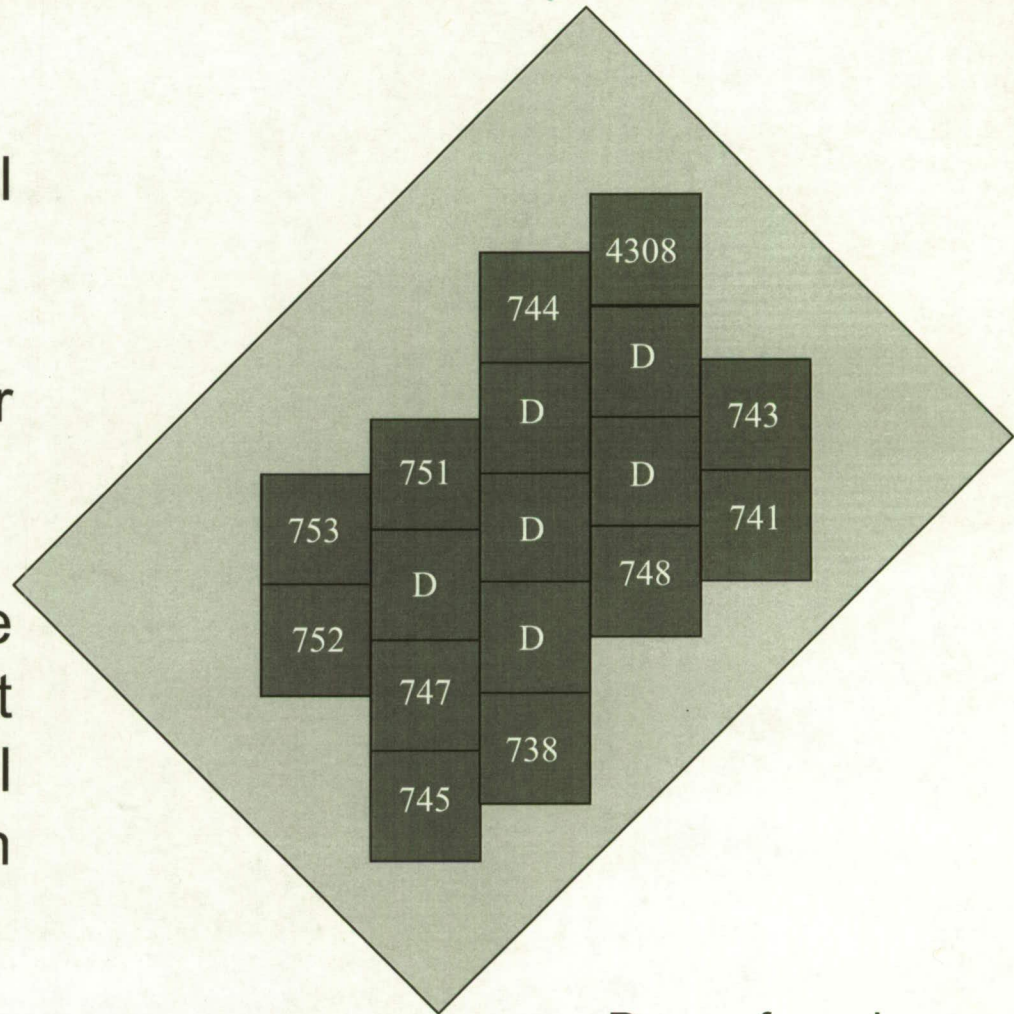
Test Panel Layout



The second test panel was a blind test.

The panel had a similar layout as the first panel.

The tiles that were scanned have the last three digits of their serial numbers displayed on the tiles on schematic



D = surface damage



Blind Panel



Site	Pit	Approximate Pit Depth, inches	Pit Diameter, inches
1	B	0.0015-0.0021	0.6
2	D	0.0198-0.0243	0.6
3	C	0.0144-0.0174	0.1
4	A	0.0030-0.0036	0.1
5	B	0.0014-0.0029	0.6
6	E	0.0074-0.0082	0.3
7	B	0.0021-0.0032	0.6
8	C	0.0112-0.0124	0.1
9	A	0.0022-0.0024	0.1
10	A	0.0017-0.0039	0.1
11	E	0.0043-0.0044	0.3
12	E	0.0072-0.0087	0.3
13	B	0.0018-0.0036	0.6

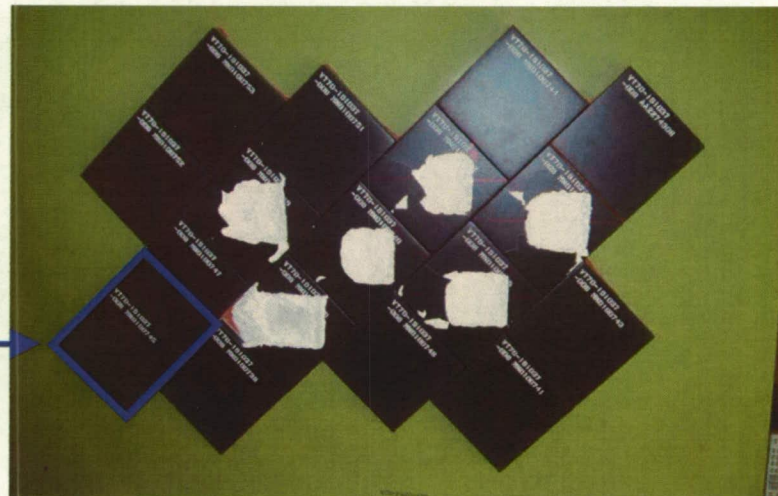
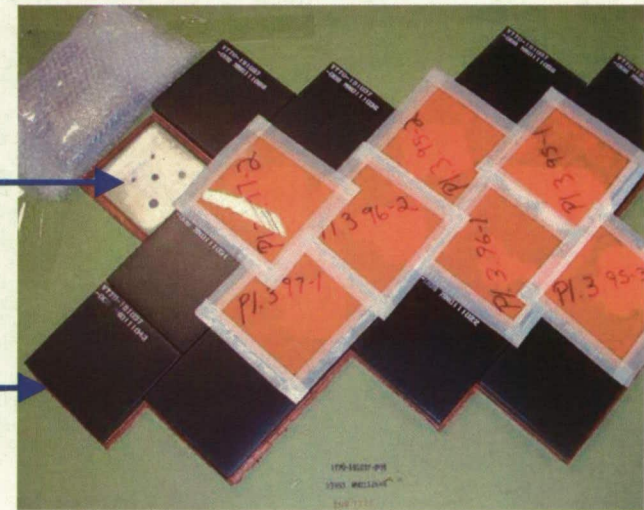
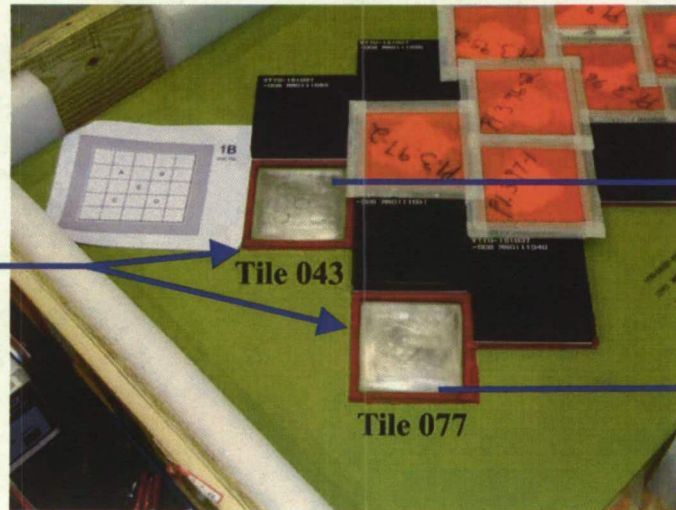
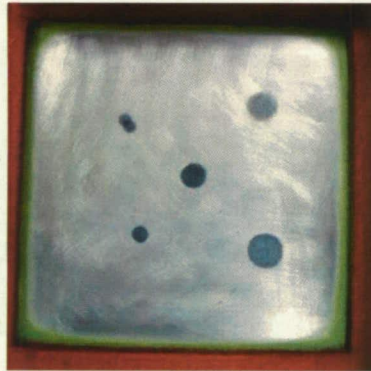


B	D	C	A	B
E	B	C	A	A
E	E	B	C	B
E	A	D	D	C
D	D	C	E	A

Size	Pit	Approximate Pit Depth, inches	Pit Diameter, inches
14	C	0.0256-0.0293	0.1
15	B	0.0018-0.0021	0.6
16	E	0.0098-0.0124	0.3
17	A	0.0033-0.0052	0.1
18	D	0.0119-0.0128	0.6
19	D	0.0085-0.0109	0.6
20	C	0.0104-0.0131	0.1
21	D	0.0199-0.0247	0.6
22	D	0.0173-0.0191	0.6
23	C	0.0117-0.0164	0.1
24	E	0.0053-0.0066	0.3
25	A	0.0025-0.0030	0.1



Test Panel Image

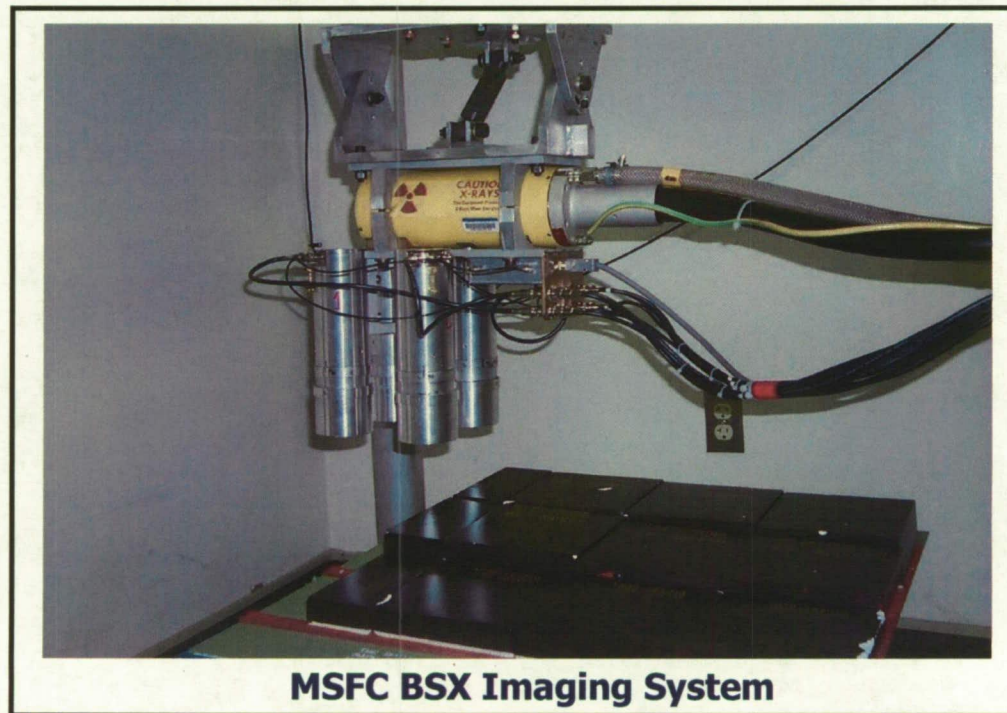




Backscatter X-ray (BSX)



- The fundamental principle of the technique is based on Compton scattering or the inelastic scattering of x-rays.
- A collimated beam of x-rays impinges on the part and the scattered radiation is measured by detectors mounted around the source.



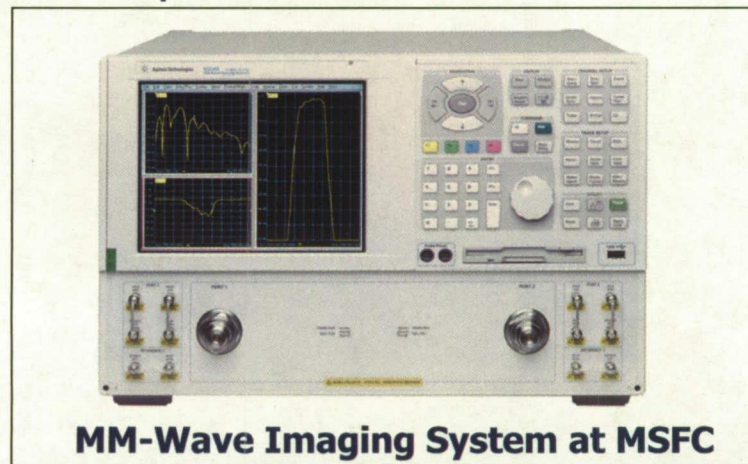
MSFC BSX Imaging System



MM-Wave Imaging



- In contrast to the BSX which operates at wavelengths of less than 1 nanometer, mm-wave imaging operates at wavelengths ranging from 1 to 10 mm
- Radio Frequency (RF) - Microwave system operates in the extremely high frequency Q-band of the electromagnetic spectrum between 30 and 300 GHz.
- System is economical and doesn't require the multitude of safety precautions that BSX requires.

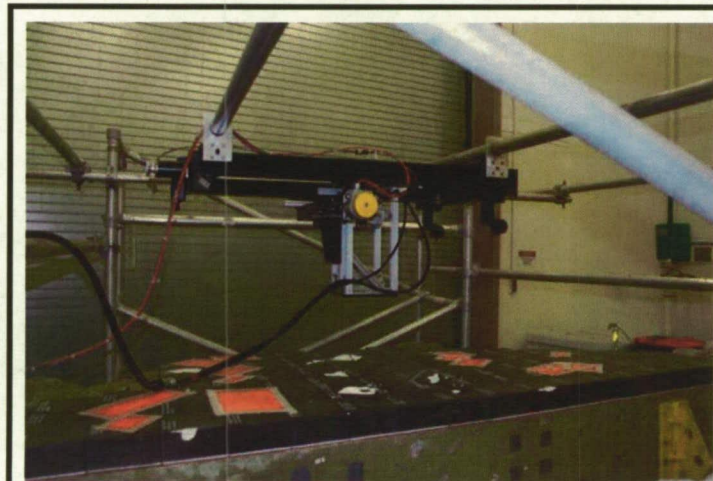




THz Imaging



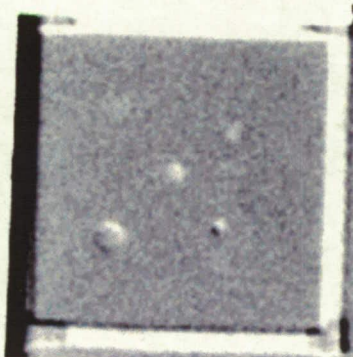
- The “Terahertz gap” forms the boundary in the electromagnetic spectrum between radio and light roughly between 300 GHz and 10 THz
- 1 Terahertz (THz) is 10^{12} cycles per second or 3 mm in wavelength
- Advances in opto-electric and semiconductor technology have enabled THz radiation to be economically generated and detected
- THz waves work well in NDE due to their high transparency in dielectric materials



THz System at KSC testing an orbiter wing mockup section



NDE Results



55 Kv, 11.6 mA,
1.1 mm focal spot

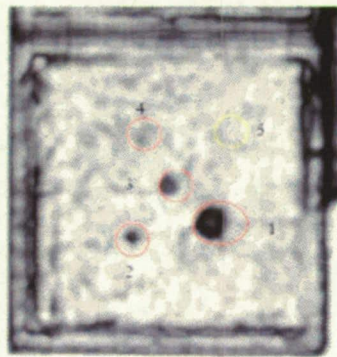
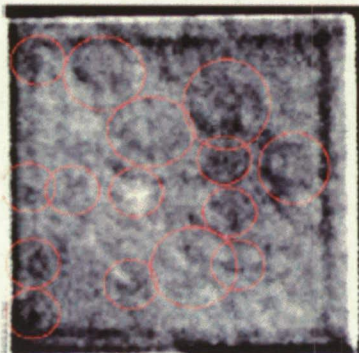
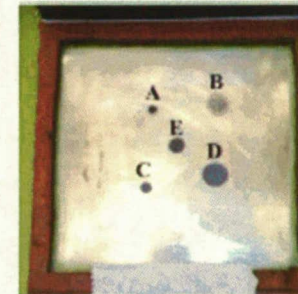
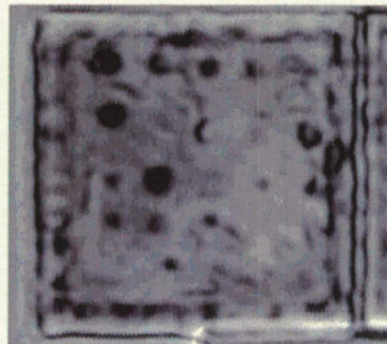


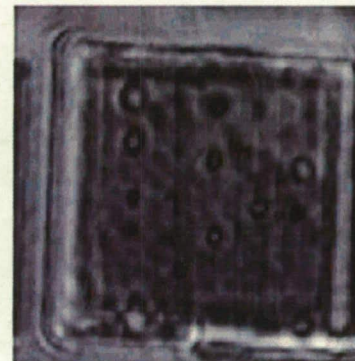
image missing



55 Kv, 40 mA,
5.5 mm focal spot



FFT at 125 GHz



Q-Band (33 to 50 GHz)



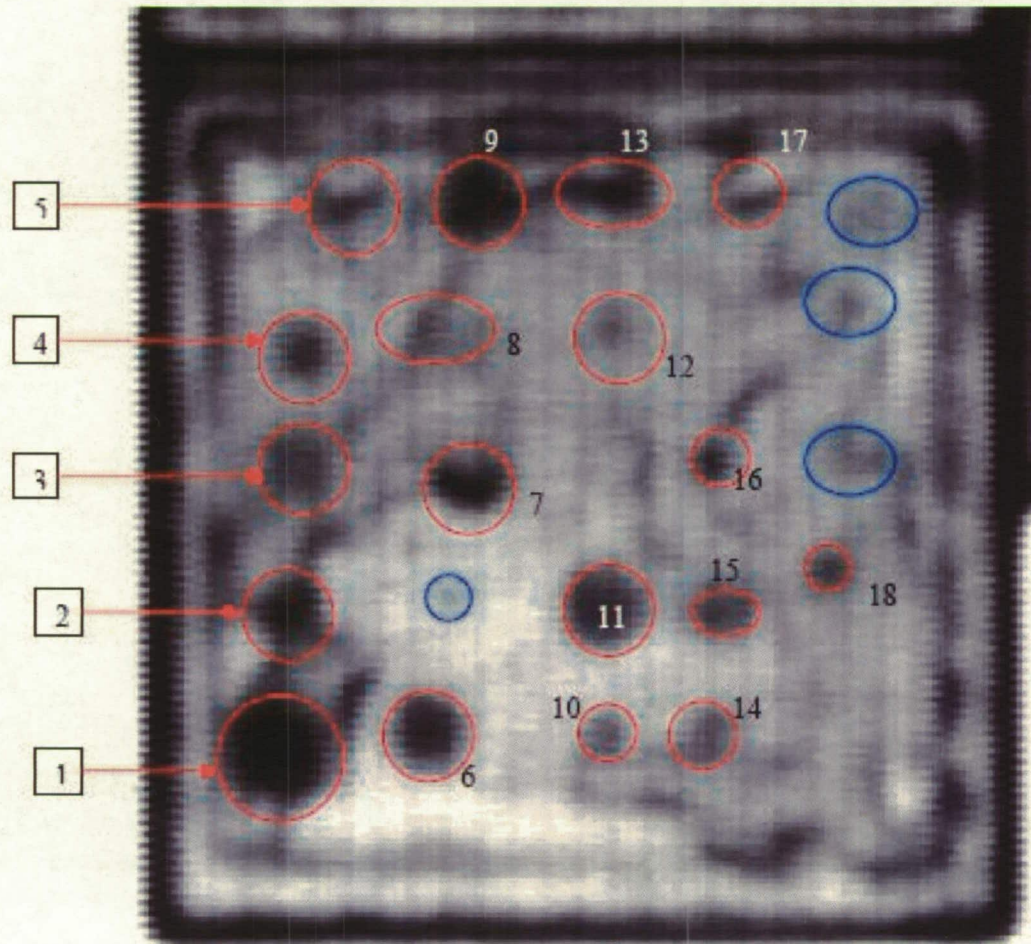
BSX
Slow (1 hr/ft²)
Poor Detection

THZ
Quick (0.5 hr/ft²)
Adequate Detection

MM-Wave (SAFT)
Slow (24hr/tile)
Not Practical (Requires moving part)



NDE Results - Terahertz



Left: Peak to Peak amplitude image from high resolution scan. Focus of 13" Zoom of 300%.

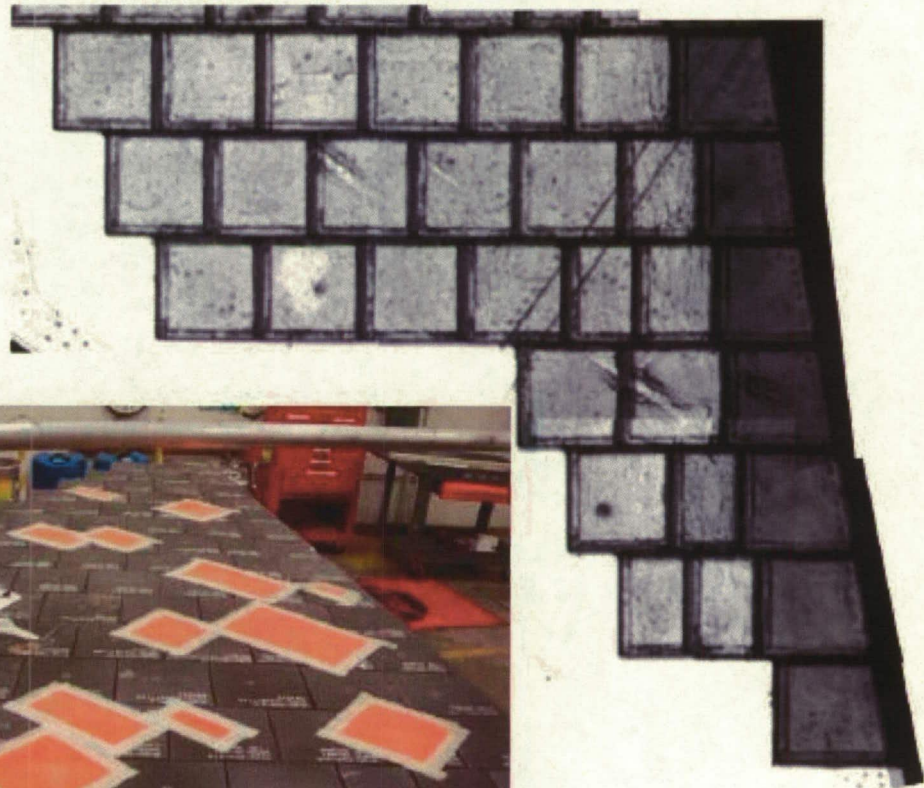
- Key**
- Corrosion Indication
 - Low Confidence Indication
 - Indication from unknown factor



NDE Results - Terahertz

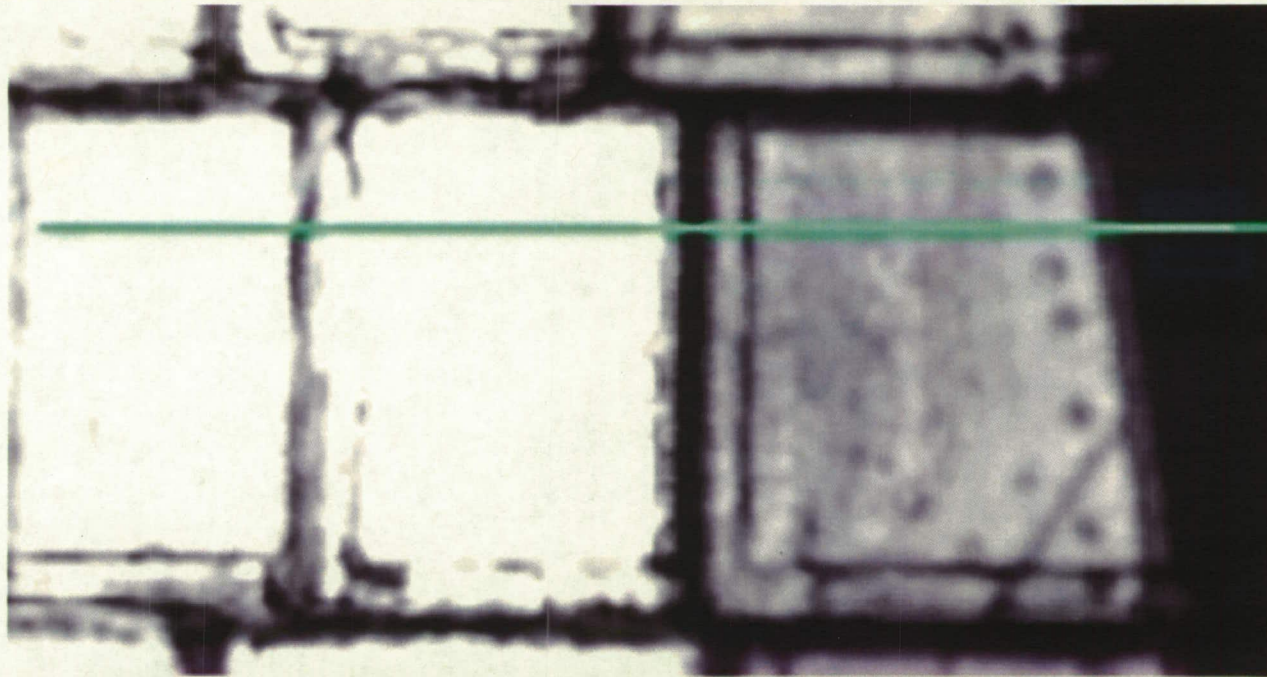


Because of the success on the test panels, the THz System was used to scan a mock wing section

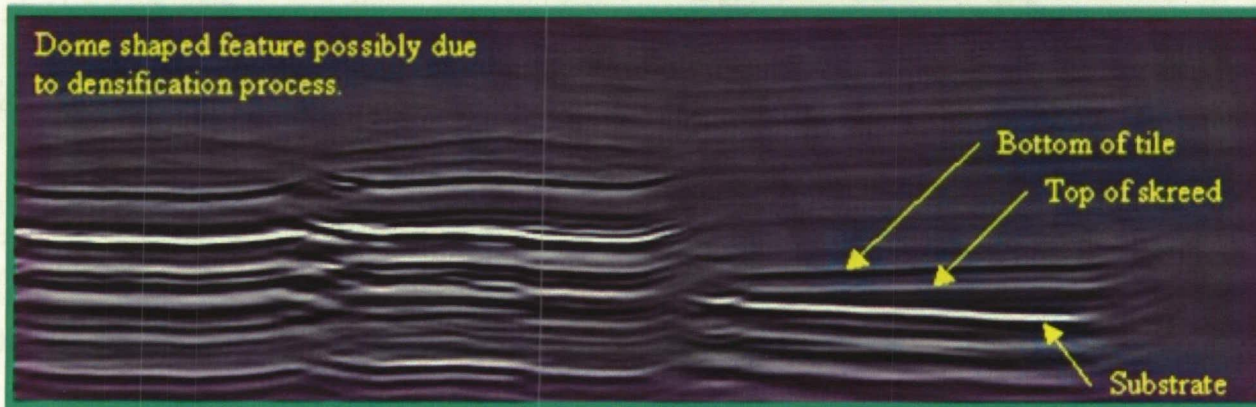




THz Imaging Results



Dome shaped feature possibly due to densification process.

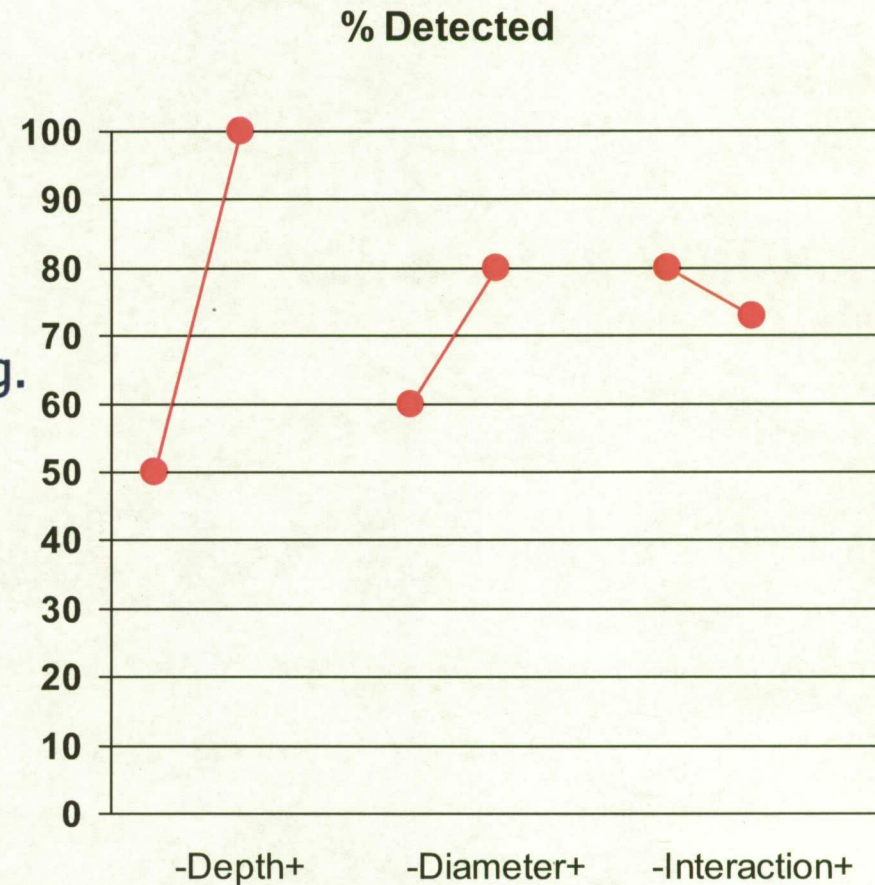




Main Effects Mean Plot



- Qualitatively, the depth of the corrosion pit is the most important factor effecting the ability to detect corrosion with terahertz and millimeter imaging.
- The interaction between corrosion area depth and diameter is not a key factor.
- As expected, the greater the depth and diameter, the more detectable the area of corrosion is.





Conclusions



- The test panels proved to be beneficial for proof of concept testing
- Inspection of the corrosion panels showed that corrosion on bare aluminum could easily be detected, however when a tile covered the corrosion, the corroded areas were more difficult to detect.
- Detection is primarily dependant on corrosion pit depth
- Measurements and analysis indicate that artificially induced corrosion areas hidden by HRSI tile with depths greater than 0.005" are detectable with Terahertz Imaging.



THE END



Many thanks to Eric Maderas, Steve Smith, Jeff Seebo, James Walker and Brad Regez for their NDE expertise.

Questions or Comments?

Experimental Design for the Evaluation of
Detection Techniques of Hidden Corrosion
Beneath the Thermal Protective System
of the Space Shuttle Orbiter

Catherine Kammerer, USA KSC

Joe Jacoby, USA KSC

Jan Lomness, NASA KSC

Paul Hintze, NASA LaRC

Rick Russell, NASA JSC